SSC21-S1-33

"Coastal marine debris mapping using multi-modal feature extraction pipeline"

Kenichi Sasaki
University of Colorado Boulder
Boulder CO; +1 7202293344
Kenichi.Sasaki@colorado.edu

Tatsuyuki Sekine, Louis-Jerome Burtz
Amanogi Corp.
Kitamagome 1-1-13, Ota, Tokyo; +81 8095482699
sekine@amanogi.space

ABSTRACT

Marine debris in the ocean is becoming an increasing problem for the management of coastal oceans and seaside resort areas. This paper presents a method for coastal marine debris mapping using satellite images from multiple satellite platforms. We carry out a pilot project in association with a local government to collect *in-situ* measurements of debris deposited on beaches and download the coincident satellite images to identify the marine debris. We propose to study the detection of marine debris on land and in the coastal ocean with various sources of satellite imagery as a way to increase the revisit frequency. High temporal resolution data can provide an agile estimation of the resources required to mitigate the pollution accumulation on the shoreline. To prevent the obscuration by cloud cover and establish high-fidelity models, we acquired the greatest number of satellite images from a variety of platforms including high temporal-resolution imagery provided by small satellite constellation programs. We first established our method using entropy of the segmentation model output on marine debris mapping in coastal areas using WorldView images provided by MAXAR corp. Then we extended the pipeline to other small satellite images using unsupervised domain adaptation techniques. We showed that the spatial representation of the segmentation map is greatly improved by the domain adaptation techniques. In addition, we confirmed the Skysat imagery provided by Planet labs can be also used in our pipeline to estimate the accumulation density of the debris, which does not require the annotated labels. This analysis shows the robust capability of this entropy pipeline to be able to map the accumulation density of debris using different types of satellite images. This extension to other images provided by various satellite platforms is also expected to increase the temporal frequency of monitoring the region of interest, which can be also applied in other remote sensing applications.

INTRODUCTION

Marine debris

Marine debris poses a serious threat to the marine environment and industry for over half a century [1]. Debris accumulation on seashores and in coastal waters results in pollution, which damages aquaculture and fisheries along with coastal recreation. This pollution requires human-resources to cleanup these coastal zones to maintain the fisheries and the tourism industry. Thus, marine pollution is estimated to result in a huge economic loss for aquaculture and tourism [2]. The comprehensive analysis of debris distribution and evolution has not been fully explored and the techniques need to be developed to evaluate the amount of debris efficiently. To this end, direct and indirect monitoring is required to collect sufficient information on the location along with its evolution in time and space. One ideal source of this monitoring information is imagery from satellite remote sensing, which can cover large areas of interest and also depict the evolution of the debris field over time. Most of the research in remote sensing application, however, only exploit satellite image data from just one satellite for their analysis [3,4]. It is known that different data have their inherent sensor bias and optical aberrations and produced by different preprocessing algorithms, which leads the analysis difficult to simply use several images together from different satellite platforms [5]. On the other hand, the combination of different satellite images drastically increases the temporal resolution of data acquisition and compensates the obscuration by cloud cover. Since we selected our target areas of interest as the southern islands of Japan, which has tropical weather conditions where typhoons or localized downpours are often observed, the optical clearness of the satellite images in that regions is often prevented by the presence of the clouds. Therefore, compensation for cloud cover is of great importance in this use case. In addition, the establishment of the multi-modal pipeline is a powerful technique to increase the temporal accuracy in other applications such as land use land classification (LULC) or satellite image time series monitoring (SITS) and the agile responses to the interested events such as natural disasters or urban changes.

Small satellite constellation programs

In recent years, small satellite usage is drastically diversified with advantages of shorter time and lower development cost. These missions in particular are occupied with Earth observation or remote sensing missions for more than 70% [6]. More and more commercial satellite constellation programs have been carried out recently and some of them have more than 100 small satellites in service for earth observation missions. Even some images provided by small satellite programs achieve sub-meter spatial resolution with much higher revisit frequency by large numbers of the constellation. This greatly increases the opportunity of the earth observation making it possible to acquire satellite images in daily basis.

DATA ACQUISITION

We carry out a pilot project in association with a local government to collect *in-situ* measurements of debris deposited on beaches and download the coincident satellite images to identify the marine debris. This cleanup data includes the recorded weight, volume and composition of the marine debris on the seashore.

We acquired a great number of satellite images to maximize the temporal resolution of the region of interests and conducted an analysis with obtained ground truth data using different types of satellite images. The analyzed images are listed in **Table 1**. We first confirmed the validity of our analysis method using the highest resolution satellite imagery: Worldview-2/3. Then, we extended the developed analysis pipeline to other image domains using unsupervised domain adaptation techniques.

Table 1: Analyzed satellite images

Satellite	Provider	Satellite size [kg]	# of sat. on orbit	Res. [m/pix]
WorldView - 2, 3	MAXAR	2800	2	0.31, 0.5
Pleiades	Airbus	970	2	0.5
Skysat	Planet labs	83-110	21	0.5
Dove	Planet labs	4 (3U)	+130	3
Nusat	Satellogic	41	18	1

METHODS AND RESULTS

Marine debris mapping

We used a semantic segmentation model designed to detect debris as an anomaly in the satellite image. The segmentation model generates the segmentation map based on the semantic segments distributed in the satellite images and the segmentation output comprises the probability distribution of defined classes. We assumed that more amounts of debris accumulate when the uncertainty of the segmentation output is higher at a specific location. Our architecture is based on a U-net model and we defined nine classes (Background, Vegetation, Trees, Buildings, Roads, Man-made structures, Water, Sand/dirt, and Rocks) to represent the semantic features in the satellite images.

We should note that most marine debris is smaller than the resolution of the satellite imagery even when we use the highest spatial resolution images making it hard to distinguish them based on its semantic patterns alone. Thus, we aim to better discriminate the features of debris based on spectral differences. The results of the segmentation model comprise the probabilities of the defined classes and the final inference result is the argument of the maxima of these nine probabilities. Even if the segmentation maps show that the coastal region comprises sand, some pixels may contain marine debris, and therefore, the uncertainty of output indicates the presence of other elements. We found that the Shannon entropy defined in eq. (**1**) can be used with this probabilistic output to quantify inhomogeneities in beaches.

$$H(C) = -\sum p_c \log p_c \qquad (1)$$

Here, $\boldsymbol{C}$ denotes the proposed semantic classes, and $\boldsymbol{p_c}$ is the probability of each class in the output of the segmentation model. We trained the model with WorldView-2/3 images and **Table 2** shows the segmentation accuracy, along with the training conditions. We visualized the segmentation map with original WorldView images in **Figure 2** and the colors in the segmentation map are defined as (Green: Trees, Light green: Vegetation, Purple: Buildings, Dark gray: Road, Light blue: Water, Yellow: Sand, Gray: Rocks). Entropy intensity map of the beaches are shown in **Figure 1**, where we know from the cleanup records that the beach in the top left is cleaned up 1 day before the satellite image was captured while the other beach in the bottom right remains dirty. We see the clear difference of entropy intensity between those two beaches. High entropy represents the high uncertainty of being 'sand', which indicates the beach is contaminated by other components. This inference result matches with the local cleanup records and this contamination is highly likely to be caused by the presence of marine debris.

Table 2: Segmentation model accuracy

# of locations	tile size [pix]	IoU	Val IoU
13	224*224	0.823	0.800

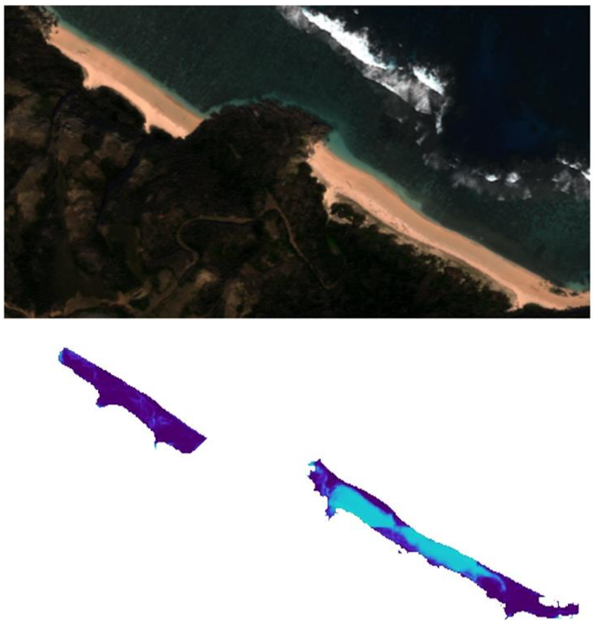

Figure 1: Original image of high-resolution satellite imagery of WorldView-3 ©2020 MAXAR TECHNOLOGIES (above) and corresponding entropy intensity map in extracted beaches (bottom)

Unsupervised domain adaptation

Once we established the debris estimation pipeline, we now focus on applying this pipeline to other datasets. First, we checked the compatibility of the segmentation model to other datasets and visualized the inference result in **Figure 3** directly generated from the model trained in MAXAR dataset using images from other satellite platforms listed in **Table 1**. This result shows the segmentation map using Airbus data even preserve the spatial representation of the semantic objects very well. On the other hand, Skysat images which have a similar spatial resolution with Airbus data does not hold the semantic features and most of the area on land is classified as 'Road'. This indicates that the image with a similar spatial resolution from original training dataset does not always show a good compatibility with them.

The results using other datasets such as Satellogic or Dove images completely collapse the spatial features in the images. This result indicates that large difference of spatial resolution leads the inference result collapsed with poor spatial representations.

Therefore, we applied the unsupervised domain adaptation techniques to improve the segmentation accuracy in other datasets. We used an adversarial training to acquire the semantic features of the images in a target domain from the model trained by the images in a source domain [7]. In this framework, we train the model as a first step using the data in source domain: WorldView images as before. And then, we train the model again using the data in target domain to generalize and adapt the trained model to the target domain. In this second training process, we prepare a discriminator network to discriminate segmentation maps generated from images in source and target domain. The discriminator uses the entropy matrix computed from the output of the segmentation model as an input and predict the domain classification output, *i.e.*, class label 1 for source and 0 for target domain, whereas the segmentation model is trained to simulate the segmentation maps of target dataset to the ones in source domain to fool the discriminator.

Eq. (3) shows the objective function of the discriminator and Eq. (3) shows the adversarial training objective of the segmentation model where $\mathcal{L}_{seg}$ represents the segmentation loss for source domain and $\mathcal{L}_{\mathcal{D}}$ is the cross-entropy domain classification loss with a weight parameter λ_{adv} and entropy matrix I_{x_t}. θ_F represents a set of parameters for the semantic segmentation model. x_s, y_s represents the images and corresponding labels in source domain whereas x_t is the images in a target domain. We implemented this adversarial training with $\lambda_{adv} = 0.1$. We also summarize the outline of this adversarial training in **Figure 4.**

$$\min_{\theta_D} \frac{1}{|\mathcal{X}_s|} \sum_{x_s} \mathcal{L}_{\mathcal{D}}\left(I_{x_s}, 1\right) + \frac{1}{|\mathcal{X}_t|} \sum_{x_t} \mathcal{L}_{\mathcal{D}}\left(I_{x_t}, 0\right) \tag{2}$$

$$\min_{\theta_F} \frac{1}{|\mathcal{X}_s|} \sum_{x_s} \mathcal{L}_{seg}(x_s, y_s) + \frac{\lambda_{adv}}{|\mathcal{X}_t|} \sum_{x_t} \mathcal{L}_{\mathcal{D}}\left(I_{x_t}, 1\right) \tag{3}$$

We show the inference result when this adversarial training is applied to each dataset in **Figure 5**.

Qualitatively, we see that all segmentation maps are greatly improved after the domain adaptation. we observe that the segmentation maps using Dove or Satellogic images have many false alarms, especially in urban regions. The segmentaion accuracy is, therefore, not sufficient to utilize this model in other remote sensing applications. Still, the inference output preserves the object boundaries and overall semantic features well even with the spatial resolution differences. On the other hand, inference result using Skysat is especially improved and reached almost a same level of spatial representation as the ones using MAXAR and Airbus data. Thus, we expect the segmentation result using Skysat data can be also utilized for our entropy pipeline.

We also adapted our entropy pipeline to Skysat images to confirm whether this approach is also applicable to the target domain. We selected three locations where we know from the cleanup records that the two of them have high density of marine debris accumulation and the rest of them does not. We show the entropy intensity map with corresponding satellite images and segmentation maps in **Figure 6**. We observe the clear difference between these 'dirty' beaches and 'clean' beach although the difference is not distinct as it was observed in the WorldView dataset shown in **Figure 1**. Thus, we confirmed the segmentation maps generated by the model adjusted by the domain adaptation techniques are applicable to the entropy pipeline using Skysat images.

The misclassifications observed in some images may be improved when we increase the number of dataset and set the different parameters for adversarial training since the previous research utilized very large datasets for their studies [7]. Thus, we still need to collect more satellite images to further improve the segmentation and debris estimation accuracy. Since we do not have annotated labels for these datasets, we evaluated the improvement of segmentation accuracy qualitatively. We need to conduct more quantitative analysis as a future work in order to determine the most accurate training parameters.

CONCLUSION

We showed the entropy metrics computed by the probabilistic outputs of the segmentation model are effective approach to estimate the accumulation density of the marine debris in coastal regions. We first confirmed the validity of the approach using WorldView images provided by MAXAR corp. and applied this model to other datasets such as Skysat by unsupervised domain adaptation. The model using Satellogic and Dove still requires more data samples and parameter tuning of the model to accurately generate the semantic segmentation maps.

We showed that the adversarial training is effective method to extend this pipeline to other satellite images. With this demonstrated technique, we can increase the temporal resolution of satellite imagery analysis by creating datasets that combine imagery obtained from several satellite platforms.

ACKNOWLEDGEMENT

This study was supported by Project Sea Unicorn by The Nippon Foundation, Japan Advanced Science and Technology Organization for education, human-resource and research (JASTO), and Leave a Nest Co., Ltd. We would also like to express our deep and sincere gratitude to the CEO of Amanogi corp., Yu Kudo for the management of this project and data acquisitions.

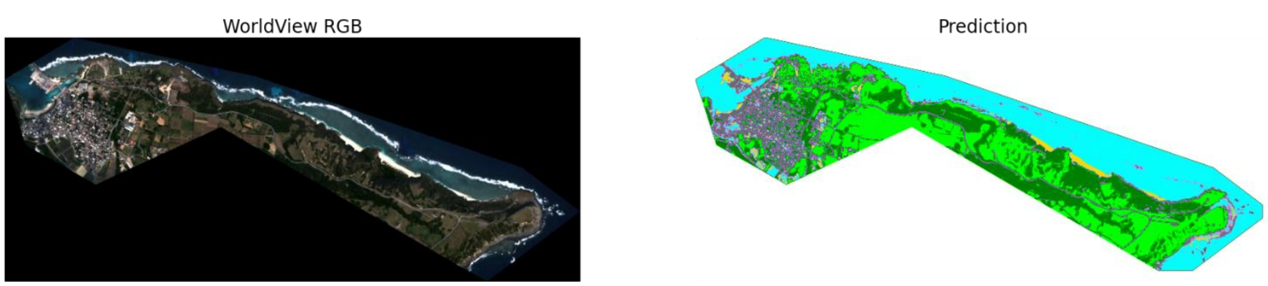

Figure 2: A semantic segmentation map (right) using WorldView images (left) ©2020 MAXAR TECHNOLOGIES

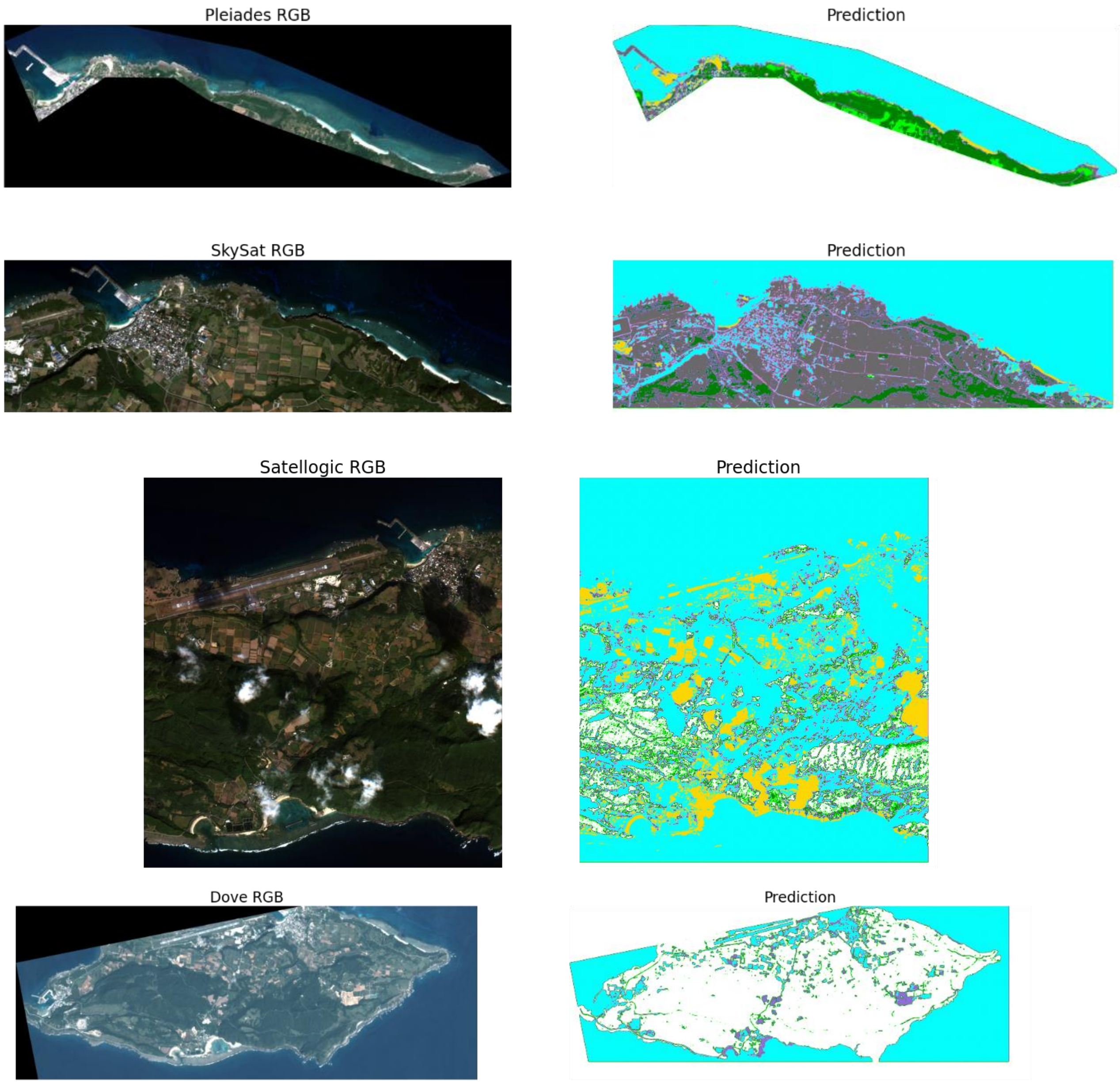

Figure 3: Inference results using satellite imagery dataset (top: Airbus ©Airbus, second top: Skysat ©Planet Labs, second bottom: Satellogic ©Satellogic, bottom: Dove ©Planet Labs) by a segmentation model trained by Worldview images

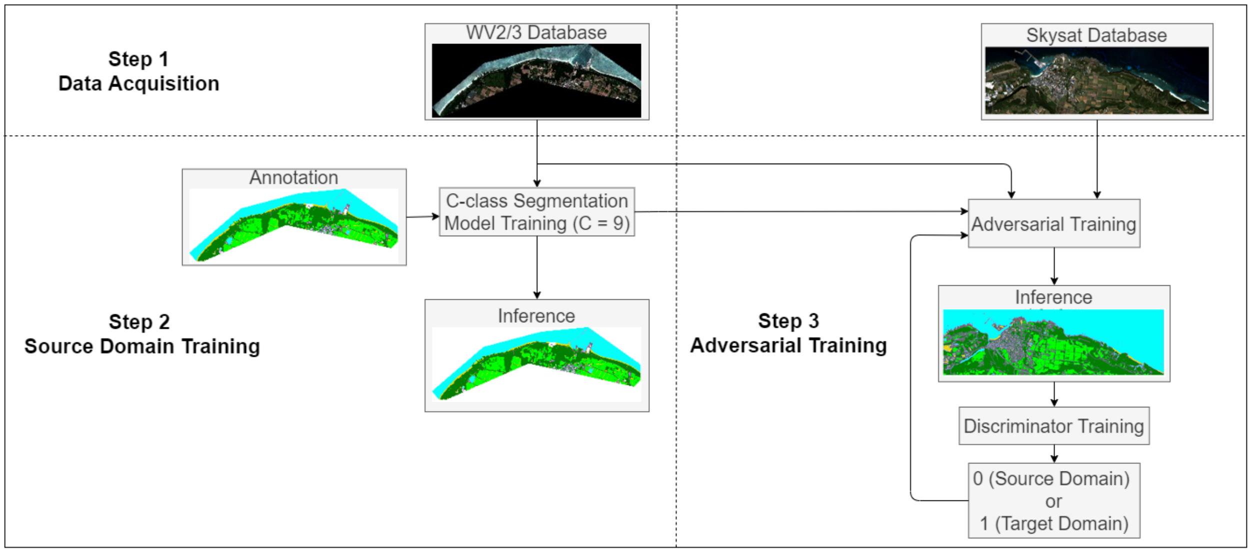

Figure 4: Overview of adversarial training steps

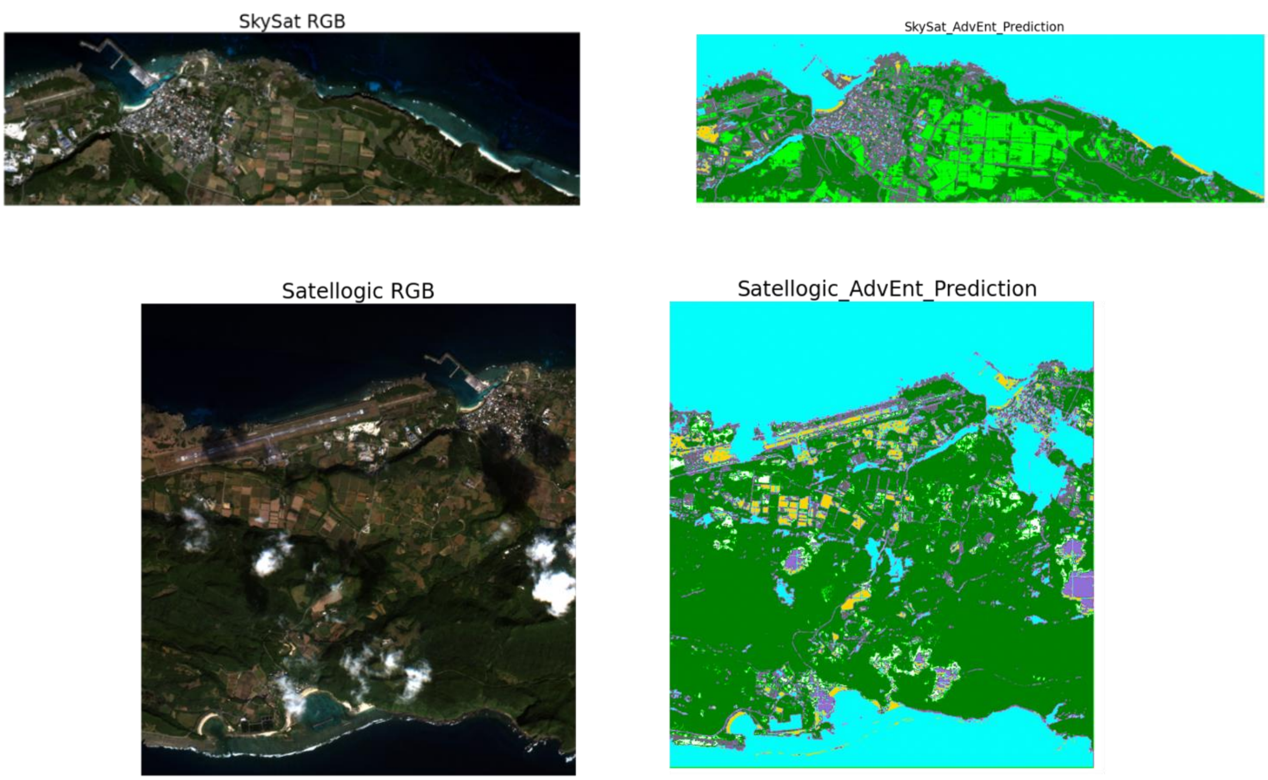

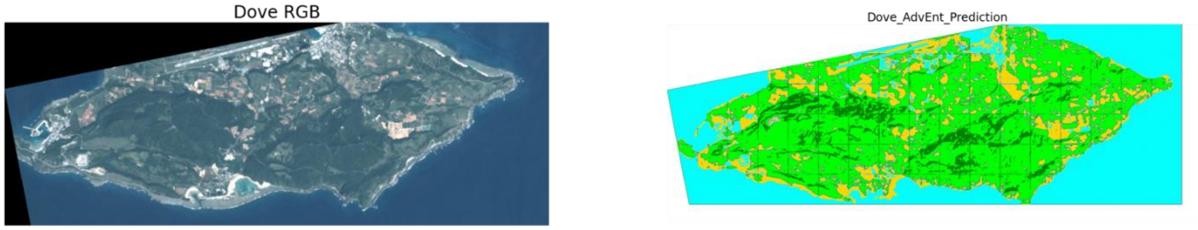

Figure 5: Inference results using other satellite imagery dataset (top: Skysat ©Planet Labs, Middle: Satellogic ©Satellogic, bottom: Dove ©Planet Labs) by an adversarial trained model

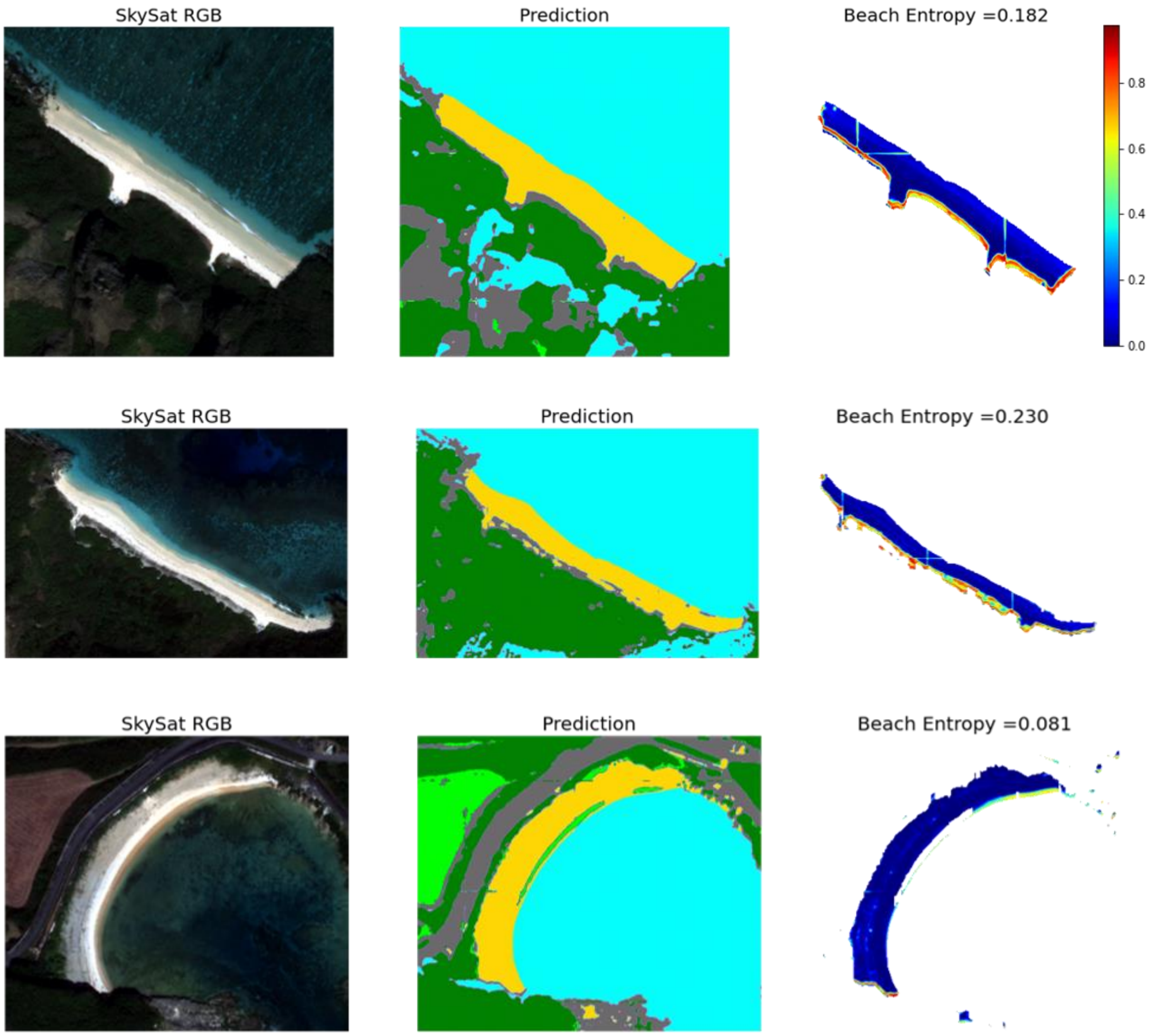

Figure 6: Beach segmentation results (middle) and the intensity maps of entropy (right) with showing the mean value of the entropy in respective beach regions (RGB images on the left ©Planet Labs). According to the cleanup records, high accumulation of marine debris is observed in the spots of the top 2 images whereas the beach in the bottom remains clean.

References

1. Keller, A. A., Fruh, E. L., Johnson, M. M., & Simon, V. (2010). Distribution and abundance of anthropogenic marine debris along the shelf and slope of the US West Coast. *60*(5), 692-70.
2. Thiel, M., Hinojosa, I., Miranda, L., Pantoja, J., Rivadeneira, M., & Vasquez, N. (2013). Anthropogenic marine debris in the coastal environment: A multi-year comparison between coastal waters and local shores. *71*(1-2), 307-316.
3. Topouzelisa, K., Papakonstantinoub, A., & Garabac, S. P. (2019). Detection of floating plastics from satellite and unmanned aerial systems (Plastic Litter Project 2018). *79*, 175-183.
4. Garaba, S., & Dierssen, H. (2018). An airborne remote sensing case study of synthetic hydrocarbon detection using short wave infrared absorption features identified from marine-harvested macro- and microplastics. *Remote Sensing of Environment, 205*, 224-235.
5. P. Teillet, G. Fedosejevs, K. Thome, and J. L. Barker, "Impacts of spectral band difference effects on radiometric cross-calibration between satellite sensors in the solar-reflective spectral domain," Remote Sensing of Environment, vol. 110, no. 3, pp. 393–409, 2007.
6. N. G. Willy, Novo, E. Moraes and Kampel, MiltonNanosatellites applied to optical Earth observation: a review. Revista Ambiente & Água [online]. 2020, v. 15, n. 3
7. T.-H. Vu, H. Jain, M. Bucher, M. Cord, and P. P´erez, "ADVENT: Adversarial entropy minimization for domain adaptation in semantic segmentation," in CVPR, 2019.